

Transformer-based Wireless Symbol Detection Over Fading Channels

Li Fan, *Graduate Student Member, IEEE*, Jing Yang, *Senior Member, IEEE*, and Cong Shen *Senior Member, IEEE*

Abstract—Pre-trained Transformers, through in-context learning (ICL), have demonstrated exceptional capabilities to adapt to new tasks using example prompts *without model update*. Transformer-based wireless receivers, where prompts consist of the pilot data in the form of transmitted and received signal pairs, have shown high detection accuracy when pilot data are abundant. However, pilot information is often costly and limited in practice. In this work, we propose the **DEcision Feedback IN-ContExt Detection (DEFINED)** solution as a new wireless receiver design, which bypasses channel estimation and directly performs symbol detection using the (sometimes extremely) limited pilot data. The key innovation in DEFINED is the proposed decision feedback mechanism in ICL, where we sequentially incorporate the detected symbols into the prompts as *pseudo-labels* to improve the detection for subsequent symbols. Furthermore, we proposed another detection method where we combine ICL with Semi-Supervised Learning (SSL) to extract information from both labeled and unlabeled data during inference, thus avoiding the errors propagated during the decision feedback process of the original DEFINED. Extensive experiments across a broad range of wireless communication settings demonstrate that a small Transformer trained with DEFINED or IC-SSL achieves significant performance improvements over conventional methods, in some cases only needing a single pilot pair to achieve similar performance of the latter with more than 4 pilot pairs.

Index Terms—Symbol Detection; Decision Feedback; MIMO; In-Context Learning; Transformer; Semi-Supervised Learning.

I. INTRODUCTION

Wireless receiver symbol detection focuses on identifying the transmitted symbols over fading channels with varying signal-to-noise ratios (SNRs). Traditional methods typically follow a two-step process: first estimating the channel using, e.g., the Minimum Mean Square Error (MMSE) estimator, and then performing symbol detection using the estimated channel. However, this approach can be computationally intensive when the system dimension is high, and is highly dependent on the quality of channel estimation. With the advance of machine learning (ML), data-driven approaches, such as deep learning models that directly learn channel estimators and symbol detectors, offer an alternative. Compared to the prior model-based, analytically driven solutions, these ML approaches have better adaptability to complex environments that have model mismatches, handle nonlinearity and system imperfections more effectively, and allow for joint optimization of multiple modules (or even the entire transceiver chain).

Despite their potential, deep learning (DL) based solutions have not been widely deployed in real-world wireless systems.

The authors are with the Charles L. Brown Department of Electrical and Computer Engineering, University of Virginia, USA. (E-mail: {lf2by, yangjing, cong}@virginia.edu.)

Among the many challenges, data dependency and generalization issues stand out as one of the most significant obstacles [1]. DL models require large amounts of diverse and high-quality training data to train, which is difficult to obtain in many wireless deployments. Poor generalization to new, unseen wireless environments (e.g., new channel conditions, interference patterns) is a particularly significant challenge due to the diverse use cases in wireless systems. Although meta-learning [2] can help with adapting to new tasks, existing approaches [3], [4] often rely on explicit model parameter updates, which increase computational complexity and reduce robustness during adaptation.

Advances in Transformer models [5], particularly decoder-only architectures like GPT [6], have driven remarkable progress in natural language processing and a broad spectrum of other domains. Recent work [7] demonstrates that pre-trained Transformers can generalize to new tasks during inference through in-context learning (ICL), without requiring explicit model updates. Specifically, the input is structured as $(y_1, f(y_1), \dots, y_n, f(y_n), y_{\text{query}})$, where (y_1, \dots, y_n) represent features in the problem domain and f is an unknown mapping. By leveraging the Transformer’s advanced next-token prediction capability, a well-pretrained model can approximate $f(y_{\text{query}})$ with high accuracy for many classes of functions, conditioned on the given context. This capability has been further validated in [8], highlighting the flexibility of Transformers in handling unseen tasks during inference.

The wireless symbol detection problem involves estimating the transmitted symbol from the received signal, where the mapping between the transmitted and received signals can be modeled as a noisy function. This formulation fits naturally with the ICL framework and Transformer-based sequence models. [9] introduces Transformers for this task using ICL, framing it as a regression problem with MSE loss and achieving near-MMSE performance. Subsequent work [10] extends this approach to multiple-input multiple-output (MIMO) systems, emphasizing the importance of task diversity during pre-training. Similarly, [11] demonstrates that Transformers are robust to pilot contamination issues in multi-user MIMO systems. While these studies focus on training relatively small Transformers from scratch, [12] proposes to leverage large language models (LLMs) to apply in-context learning. This method transforms the detection problem from a numerical task into a linguistic one, incorporating LLM calibration techniques. Collectively, these studies highlight that Transformers are powerful and versatile models, well-suited for addressing a range of challenges in wireless communication systems.

Despite these advances, prior studies face several limita-

tions. Most solutions treat symbol detection as a regression task, relying on MSE-based objectives and post-processing to map continuous outputs to discrete symbols. Furthermore, many methods require an abundance of pilot pairs to achieve reasonable performance, which may not be feasible in practice. Additionally, the use of large models incurs long delay and requires significant memory and computation resources, further limiting their applicability in real-world deployments.

Inspired by decision feedback in wireless communication (e.g., decision feedback equalizers over multi-path fading channels), we propose a novel prompt design by incorporating decision pairs. Specifically, we combine the current received signal with the model’s detected symbol in a pair, merging them with previous prompts to form a new, larger prompt for subsequent symbol detection. Our DEFINED model employs a carefully designed mixture training process to achieve high performance with limited pilots (sometimes as few as a single pilot) while maintaining accuracy when sufficient pilots are available. Additionally, we frame the problem from a semi-supervised learning (SSL) perspective by developing a new IC-SSL model. This model demonstrates that Transformers can extract information from both labeled pairs and unlabeled features, enabling in-context semi-supervised learning during inference with both supervised data pairs and partially observed data in the prompt. This result highlights the promising potential of Transformers in future wireless communication systems. Extensive experiments across various modulation schemes and channel distributions validate the effectiveness of our approach. We summarize our contributions as follows:

- We propose a novel Transformer model that jointly performs channel estimation and symbol detection. Our key innovation in the DEFINED model is the incorporation of decision feedback to allow pseudo-labels to be used in conjunction with the limited pilot data, to gradually increase the effective context length and thus improve the output performance.
- We develop a mixture training process for DEFINED, achieving significant performance improvements with very limited pilot data while maintaining high accuracy with sufficient pilot data, making the model adaptable to practical scenarios.
- We propose an IC-SSL detector as an alternative of DEFINED. IC-SSL demonstrates that Transformers can extract information from both labeled pairs and *unlabeled* features to make accurate detections. This highlights the ability of Transformers to perform ICL from *partial* observations, which showcases its great potential for wireless applications.
- We conduct extensive experiments across various modulation schemes in both SISO and MIMO systems under varying configurations, where we show that a very small Transformer model trained by DEFINED and IC-SSL can achieve strong accuracy and generalization performance.

The remainder of this paper is organized as follows. Section II reviews the related work. Section III presents the system model and canonical methods. Section IV introduces in-context learning-based symbol detection. The proposed DEFINED method, including model structure and training details, is described in Section V, with an IC-SSL enhance-

ment detailed in Section VI. Section VII presents experimental results, and Section VIII concludes the paper.

II. RELATED WORK

Machine learning has become a crucial tool for wireless system designs [13]–[18]. For channel estimation and symbol detection, [19], [20] propose variational autoencoders (VAEs), while deep learning architectures such as Convolutional Neural Network (CNN) and Recurrent Neural Network (RNN) have been explored to improve channel estimation [21]–[23]. CNN-based models effectively approximate the MMSE estimators [22], and end-to-end CNN frameworks jointly perform channel estimation and symbol detection [24].

The Transformer model [5] has become fundamental across various fields. GPT-2 extends Transformers for multitask learning [6], while GPT-3 introduces in-context learning (ICL), allowing adaptation solely through contextual inputs [7]. Unlike meta-learning, ICL does not require parameter updates, making it well-suited for wireless applications. Theoretical studies reveal that Transformers approximate regression tasks [8] and perform Bayesian inference [25]. Pre-training on diverse tasks enhances ICL performance [26], and Transformers exhibit implicit gradient descent during ICL, optimizing predictions without updating parameters [27], [28]. Research also highlights the importance of input structure, showing that distribution, label space, and structural cues significantly influence ICL performance [29], [30].

ICL has been applied to wireless tasks such as channel estimation and resource allocation. [9] first introduced Transformers for symbol detection, demonstrating their effectiveness as in-context estimators. [10] extended this to MIMO systems, highlighting threshold behavior in ICL with increasing pre-training tasks, while [11] explored multi-user cell-free MIMO systems. Large language models (LLMs) have also been adapted for wireless applications, including resource management and network configuration. [12] applies ICL-based LLMs for symbol detection, while [31], [32] propose WirelessLLM and WirelessAgent frameworks, respectively, leveraging knowledge alignment and multimodal data fusion. Unlike these approaches, our work focuses on training a Transformer-based receiver from scratch. Additionally, Transformers have also been used for radio fingerprinting [33], automatic modulation recognition (AMR) [34], spectrum sensing [35], and neuromorphic designs aimed at reducing power consumption [36]. Contrastive semi-supervised learning has improved AMR with fewer labeled samples [37].

III. SYSTEM MODEL AND CANONICAL METHODS

A. Wireless Model

To more clearly illustrate our design, we consider a canonical receiver symbol detection problem over a standard narrowband wireless fading channel. Broadly, we consider an (N_t, N_r) MIMO system, where the channel is represented by an $N_r \times N_t$ complex-valued matrix H_t at time t , following a distribution P_H . We do not specify the channel distribution but normalize the channel coefficients such that each entry in H_t

has a unit variance. The received signal at time t is expressed as:

$$y_t = H_t x_t + z_t,$$

where the channel noise $z_t \in \mathbb{C}^{N_r}$ is modeled as a complex additive white Gaussian noise vector with zero mean and covariance matrix $\sigma^2 I$. Each entry of the input vector $x_t \in \mathbb{C}^{N_t}$ is sampled uniformly at random from a constellation set \mathcal{X} (e.g., 16QAM), and this modulation process is independently and identically distributed (i.i.d.) across both time and space. We normalize the signal to ensure a unit average total transmit power, i.e., $\mathbb{E}[\|x_t\|^2] = 1$. The average signal-to-noise ratio (SNR) at any receive antenna is thus given by $\text{SNR} = 1/\sigma^2$.

We focus on the *block-fading* channel model [38] in this paper, illustrated in Figure 1. In this model, the channel H_t remains constant over a coherent time period of T time slots, and is i.i.d. across different coherence periods. In other words, $H_t = h_l, \forall t = (l-1)T + 1, \dots, lT$, for the l -th coherence period where h_l is drawn i.i.d. from P_H . Correspondingly, the data transmission is organized into frames, where each frame has a length that is at most T . The frame structure is designed such that the first k transmitted symbols are known and pre-determined *pilot symbols*, whose original purposes include assisting the receiver to perform channel estimation [39] of h_l so that it can perform coherent symbol detection. Generally speaking, based on the reception of a few pilot pairs $D_k = \{(y_1, x_1), \dots, (y_k, x_k)\}$, The goal is to design a demodulator that accurately recovers the transmitted symbols x_{k+1}, \dots, x_T from the received signals y_{k+1}, \dots, y_T with high probability while maintaining reasonable complexity.

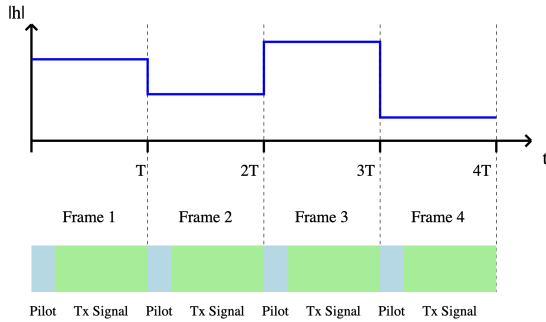


Fig. 1. Illustration of block-fading channels and the associated frame structure. In each frame, the channel remains constant and the frame is divided into pilot signals and transmit data signals.

B. Canonical Methods for Coherent Symbol Detection

In the traditional approach, the receiver first estimates the channel using pilot signals, then performs symbol detection on the received signal y_t via hypothesis testing for each $t = k + 1, \dots, T$. Typically, the (Linear) MMSE estimator is used for channel estimation, which is given by $\hat{H} = YX^\dagger(XX^\dagger + \sigma^2 I)^{-1}$, where $X = [x_1, x_2, \dots, x_k] \in \mathbb{C}^{N_t \times k}$ is the pilot matrix and $Y = [y_1, y_2, \dots, y_k] \in \mathbb{C}^{N_r \times k}$ is the received signal matrix. Then, with the estimated channel, the transmitted symbol \hat{x}_t is detected by projecting y_t onto the closest symbol in the modulation constellation \mathcal{X} as $\hat{x}_t = \arg \min_{x \in \mathcal{X}} \|\hat{H}x - y_t\|^2, \forall t = k + 1, \dots, T$.

This two-step process treats channel estimation and symbol detection as separate tasks. Such decoupling can result in

suboptimal detection, particularly under noisy conditions or limited pilot data [39]. Optimal estimators like MMSE rely on precise statistical models of the channel and noise, which can be difficult to obtain for complex wireless environments. These estimators are also computationally intensive due to matrix inversions and posterior probability calculations, making them less appealing for real-time high-dimensional systems.

To address these challenges, data-driven methods [15] have been explored for joint channel estimation and symbol detection. Deep learning architectures have shown promise [4], [21]–[24], [40], but their high data requirements [41] and poor adaptability to varying channel conditions without retraining limit their real-world applicability [1].

IV. IN-CONTEXT LEARNING-BASED SYMBOL DETECTION

ICL for symbol detection leverages the structure of wireless communication frames, particularly in block-fading channels where channel conditions remain stable during the coherence time. Within each frame, pilot signals are followed by subsequent received signals, which naturally align with the Transformer architecture’s strength in processing *sequence-based inputs*. The Transformer’s ability to model dependencies among sequential data allows it to capture complex relationships within transmitted signals, making it highly effective for symbol detection tasks.

In this section, we introduce the ICL-based symbol detection method. We first formulate the symbol detection problem, and then present the ICL implementation using a popular Transformer model GPT-2, which also serves as the backbone of our proposed solution¹.

A. ICL-based Problem Formulation

Each ICL symbol detection task τ corresponds to a latent channel H and a channel noise level σ^2 , drawn from the unknown joint distribution $P_\tau = P_H P_{\sigma^2}$. The ICL-based symbol detection does not have prior knowledge of the specific task τ , meaning it does not know the current channel realization H or the SNR level $1/\sigma^2$. Instead, it is only provided only with a prompt $S_k^\tau = (D_k^\tau, y_t)$, consisting of k target pairs $D_k^\tau = \{(y_1, x_1), \dots, (y_k, x_k)\}$, which are sampled from the conditional distribution $P_{x,y|\tau}$ and serve as the in-context examples for the current task τ , along with the query $y_t, \forall t = k + 1, \dots, T$.

As previously mentioned, each context pair (x_i, y_i) and the query pair (y_t, x_t) are i.i.d. samples given task τ . For block-fading channels, the context set D_k^τ , also referred to as *pilot signals* in wireless communication, enhances the channel estimation, thereby improving the reliability and accuracy of data transmission. We note that a significant advantage of the proposed solution is that there is no need to change the existing frame structure or the design of pilot signals. Rather, the innovation is entirely at the receiver side where we leverage the pilot and decoded signals in a different way. This is an

¹We use GPT-2 with elaborated design choices as a concrete example throughout the paper. However, the proposed principle can be easily adapted to other Transformer architectures.

important advantage in practice as it allows for (backward) compatibility with the existing standard.

The goal of symbol detection is to identify the corresponding input signal x_t for the new query signal y_t from the same task. The ICL-based detection makes its decision as $\hat{x}_t = f_\theta(S_t^\tau)$, where θ represents the parameters of the model. The detection for the query is measured by the Symbol Error Rate (SER), which is the frequency at which transmitted symbols are incorrectly decoded. The expected SER for the new query with k contexts, taking the expectation over the task distribution for $\forall k = 1, \dots, T - 1$, is defined as:

$$\text{SER}_k(\theta) = \mathbb{E}_\tau \mathbb{E}_{D_k^\tau, y_t | \tau} [f_\theta(D_k^\tau, y_t) \neq x_t]. \quad (1)$$

B. Vanilla In-Context Symbol Detection

Transformer models have emerged as powerful tools for classification tasks [42], leveraging their ability to capture long-range dependencies. This approach to wireless symbol detection was introduced in [9], [10]. The input-output structure is illustrated in Figure 2. With a causal masked self-attention mechanism, the model outputs the detection \hat{x}_t at the corresponding position of y_t , relying only on known preceding contexts and the received signal. During the forward process, the Transformer solves $k + 1$ detection problems for the same task τ , using an increasing number of pilot data points. The results in [9], [10] demonstrate that the Transformer exhibits strong capabilities in symbol estimation within context, without requiring explicit model updates.

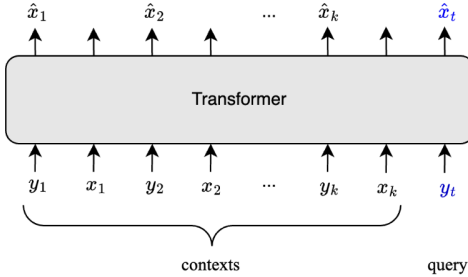


Fig. 2. Decoder-only Transformer architecture for ICL-based symbol detection with k pilots. Detection output applies to $t = k + 1, \dots, T$.

V. DECISION FEEDBACK IN-CONTEXT DETECTION

The vanilla ICL approaches for symbol detection require sufficient context to achieve accurate estimation, which is often impractical in real-world scenarios. Pilot signals are costly and limited, reducing their adaptability for practical applications. Furthermore, adding more pilot signals reduces the amount of slots for data transmission, effectively reducing the system throughput. For situations where the number of pilots is small, neither conventional two-stage (channel estimation then symbol detection) nor vanilla ICL solutions can achieve good performance. Additionally, these approaches generally formulate the symbol detection task as a *regression* problem, as in [10], [11], [26], where a Transformer model is trained to minimize the MSE loss. Although their models achieve performances comparable to the optimal MMSE estimator for x , an additional projection step is required to map the output to the appropriate transmitted symbol, leading to a mismatch and losing optimality in the process.

In contrast, we directly formulate the problem as a *multi-class classification* task [42], allowing the model to perform symbol detection while directly optimizing for SER during inference. This approach eliminates the need for explicit channel estimation, as the model implicitly gains knowledge of the channel through the pilot signal pairs. Additionally, we generalize the approach to effectively handle scenarios where pilot information is highly limited by sequentially feeding back the already decoded symbol pairs as *noisy pilots* and incorporating them as part of the prompt. Our model demonstrates robust performance even in challenging conditions with only a *single* pilot, outperforming previous ICL models that struggle with insufficient pilot data. At the same time, it maintains high accuracy when sufficient pilot data is available.

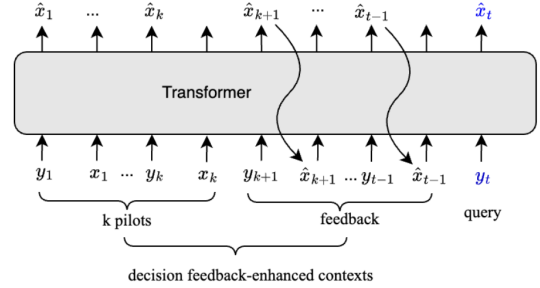


Fig. 3. DEFINED model architecture with k pilots and $(t - k - 1)$ decision feedback contexts to detect $x_t, \forall t = k + 1, \dots, T$.

Inspired by the decision-feedback concept in wireless communication, we propose the DEcision FEedback IN-ContEXt DEtectION (DEFINED) method for symbol detection, as illustrated in Figure 3. The key innovation is that the DEFINED model extends the prompt by incorporating the previously received signals and detection decisions alongside prior prompts to improve subsequent detections. While traditional decision-feedback equalizers (DFEs) address inter-symbol interference (ISI), our study focuses on narrowband channels without ISI. Nevertheless, decision feedback is effective here due to the latent common channel. Noisy feedback also provides valuable information, further improving model detection.

Next, we provide a detailed description of the DEFINED model structure and explain its data processing flow. Specifically, we highlight the critical role of the multi-head self-attention mechanism in enabling efficient information extraction. Furthermore, we discuss the model's size and describe the training process, which comprises dedicated pre-training and fine-tuning phases, as outlined in the following subsections.

A. Tokenization, Attention, and Detection

We delve into the implementation of the Transformer for symbol detection, focusing on signal processing and its most significant components, the self-attention mechanism, as illustrated in Figure 4. The computation involves several key steps.

First, tokenization converts the input IQ samples into embeddings, which are then processed through L cascaded layers of the decoder backbone, adapted from the GPT-2 model. The model employs masked multi-head self-attention, a pivotal operation in Transformer architectures. This attention mechanism enables the output embeddings to capture long-range dependencies and extract relevant information from the

input sequence. In the context of symbol detection, these dependencies represent the relationships between earlier pilot pairs and the current detection task involving the received query signal, both of which depend on the same channel h_l in the block fading model. Capturing these relationships is critical for learning signal characteristics and the underlying channel structure, ultimately improving detection accuracy.

Following the self-attention step, the Transformer's output passes through a classification head consisting of a linear transformation, which projects it into the classification dimension. Finally, a softmax layer computes the class probabilities, and the class with the highest probability is selected as the detected symbol. Each component is explained in detail below.

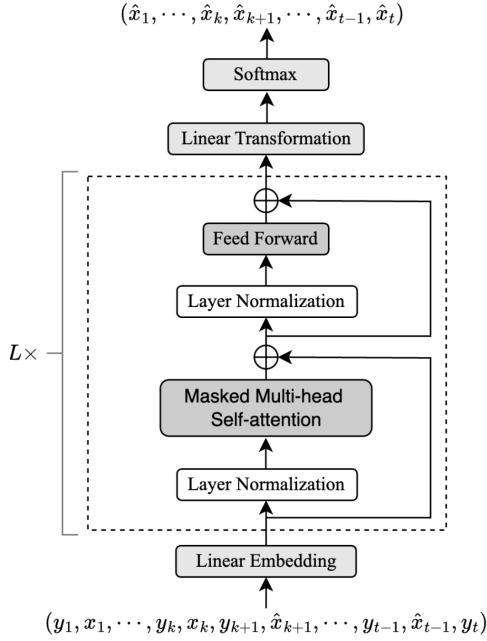


Fig. 4. DEFINED model architecture featuring linear embedding for tokenization, L cascaded decoder layers, and a classification head.

1) *Linear Embedding*: The first step in the data processing pipeline is tokenization, which converts the IQ samples into input embeddings. Both the transmitted and received signals are complex. For the received signal $y \in \mathbb{C}^{N_r}$, we concatenate its real and imaginary parts as $\tilde{y} = [\text{Re}(y), \text{Im}(y)] \in \mathbb{R}^{2N_r}$, where $\text{Re}(y)$ and $\text{Im}(y)$ represent the real and imaginary parts of the complex signal, respectively.

For the transmitted signal $x \in \mathbb{C}^{N_t}$, where each symbol is sampled from a discrete constellation set with size C , we represent each signal using one-hot encoding: $\tilde{x} = \text{Onehot}(x) \in \mathbb{R}^{CN_t}$.

Next, we apply zero padding to ensure uniform dimensionality $D_s = \max(2N_r, CN_t)$. The input is then passed through a linear embedding layer parameterized by a learnable matrix $A \in \mathbb{R}^{D_e \times D_s}$. The resulting embedding sequence is $E = [A\tilde{y}_1, A\tilde{x}_1, \dots, A\tilde{y}_t]$, which converts the input signals into a unified embedding space for further processing by the Transformer backbone.

2) *Decoder Layers with Masked Multi-Head Attention*: Our model adopts the GPT-2 backbone with L stacked decoder layers, where each layer refines the representation of the input

sequence: $E^{(0)} = E, E^{(\ell+1)} = \text{DecoderLayer}(E^{(\ell)})$, $\ell = 0, \dots, L-1$.

Each decoder layer consists of masked multi-head attention (MHA), a feedforward network (FFN), and residual connections with layer normalization. GPT-2 employs a pre-normalization scheme, where layer normalization is applied before each sub-layer [6]. The forward pass computation of the Transformer follows a standard process, which we summarize here for completeness.

a) *Masked Multi-Head Attention (MHA)*: MHA captures long-range dependencies across the input sequence, which, in our case, is established via the common channel h_l . Given the normalized input: $\tilde{E}^{(\ell)} = \text{LayerNorm}(E^{(\ell)})$, queries (Q), keys (K), and values (V) are computed as: $Q = \tilde{E}^{(\ell)}W_Q$, $K = \tilde{E}^{(\ell)}W_K$, $V = \tilde{E}^{(\ell)}W_V$. To enforce autoregressive behavior, a causal mask M prevents attention to future tokens: $\text{MaskedAttention}(Q, K, V) = \text{softmax}\left(\frac{QK^T}{\sqrt{d_k}} + M\right)V$. Outputs from multiple attention heads are concatenated and linearly projected: $\text{MHA}(\tilde{E}^{(\ell)}) = \text{Concat}(\text{head}_1, \dots, \text{head}_h)W_O$. A residual connection is then applied: $U^{(\ell)} = E^{(\ell)} + \text{MHA}(\tilde{E}^{(\ell)})$.

b) *Feedforward Network (FFN)*: The FFN processes the intermediate output through two linear transformations with a ReLU activation: $\text{FFN}(\tilde{U}^{(\ell)}) = \text{ReLU}(\tilde{U}^{(\ell)}W_1 + b_1)W_2 + b_2$. A residual connection produces the final layer output: $E^{(\ell+1)} = U^{(\ell)} + \text{FFN}(\text{LayerNorm}(U^{(\ell)}))$. Pre-normalization stabilizes training, as shown in [6].

3) *Classification Layer*: The final decoder output, $E^{(L)}$, is projected onto the classification space, where a softmax function determines the most likely transmitted symbol: $\hat{x} = \arg \max(\text{softmax}(W_c E^{(L)}))$, where W_c is the classification weight matrix.

B. Model Parameters

Our specific Transformer model is designed with an embedding dimension of $d_e = 64$, $L = 8$ layers, and $h = 8$ attention heads, resulting in approximately **0.42 million** parameters, which is significantly smaller compared to large language models (LLMs) commonly applied in wireless communication tasks, such as those discussed by [12], [31]. For instance, even LLMs like GPT-J 6B contain over 6 billion parameters, making them approximately 14,000 times larger than our model. This compact size not only enables deployment on edge devices but also significantly shortens the inference time, enabling low-latency detection at the receiver.

C. Training Details

In this section, we describe our data generation process and the training of the DEFINED model. Training includes a pre-training phase to equip the model with general predictive abilities and speed up convergence, followed by fine-tuning to adapt the model to scenarios with limited pilot data.

1) *Data Generation*: We generate data according to the wireless communication model described in Section III-A. Specifically, we consider both SISO and 2x2 MIMO systems and explore various modulation schemes, including BPSK, QPSK, 16QAM, and 64QAM. For each wireless system and

modulation task, we generate prompts consisting of sequences with T pairs, where the maximum sequence length is set to $T = 31$. Both systems operate under a Rayleigh block-fading channel, with the channel coefficient sampled as $H \sim P_H = \mathcal{CN}(0, 1)$ and remaining constant over each block. The channel noise is sampled i.i.d. from a Gaussian distribution $z_t \sim \mathcal{CN}(0, \sigma^2 I)$. Within each block, the noise variance σ^2 is constant and shared across all noise samples. However, for different blocks, σ^2 is i.i.d. sampled from a uniform distribution P_{σ^2} over the range $[\sigma_{\min}^2, \sigma_{\max}^2]$. Varying noise levels during training enhances generalization by exposing the model to diverse channel conditions. Sampling σ^2 from a distribution instead of fixing it to a specific SNR improves adaptability to interference, increasing reliability in practical deployments. This variability applies only during training, while evaluation is conducted at fixed SNR levels for controlled performance assessment. The training batch size is set to 512.

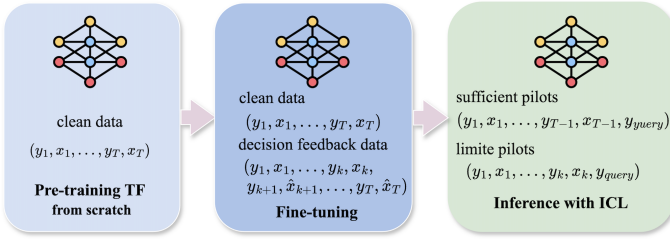


Fig. 5. The training process includes pre-training on clean data, followed by fine-tuning on a mixed dataset of clean and decision feedback noisy data. The model demonstrates strong performance, adapting to both limited and sufficient pilot scenarios during symbol detection (i.e., inference).

2) *ICL Pre-training*: We delve into the details of model training, which is divided into two phases, as illustrated in Figure 5. First, we define **ICL-training** and **ICL-testing** as the corresponding operations on ground-truth data, represented by the clean prompt for $t = 1, 2, \dots, T$: $S_t^{\text{ICL}} = \{y_1, x_1, \dots, y_{t-1}, x_{t-1}, y_t\}$.

On the other hand, **DF-training** and **DF-testing** utilize iteratively decoded sequences with k pilot data and model decision feedback, operating on the decision feedback prompt for $t = k + 1, \dots, T$: $S_t^{\text{DF}} = \{y_1, x_1, \dots, y_k, x_k, y_{k+1}, \hat{x}_{k+1}, \dots, y_{t-1}, \hat{x}_{t-1}, y_t\}$. Each estimation \hat{x}_j for $j = k + 1, \dots, t - 1$ is the model output, which depends on the first k pilot points and preceding model decisions. This output evolves during model training and gradually converges as training progresses.

We next define the loss functions for ICL-training and DF-training. The adopted loss function is the cross-entropy loss between the model's output and the ground-truth labels, defined as: $\text{loss}(\hat{x}, x) = -\sum_{c \in \mathcal{X}} \mathbb{1}(x = c) \log P(\hat{x} = c)$, where \hat{x} is the predicted output, x is the ground-truth symbol, \mathcal{X} represents the modulation constellation set, and $\mathbb{1}(\cdot)$ is the indicator function.

Using this loss definition, the loss functions for ICL-training and DF-training are formulated as:

$$\mathcal{L}^{\text{ICL}}(\theta) = \frac{1}{NT} \sum_{i=1}^N \sum_{t=1}^T \text{loss}(f_{\theta}(S_{t,i}^{\text{ICL}}), x_{t,i}), \quad (2)$$

$$\mathcal{L}^{\text{DF}}(\theta) = \frac{1}{N(T-k)} \sum_{i=1}^N \sum_{t=k+1}^T \text{loss}(f_{\theta}(S_{t,i}^{\text{DF}}), x_{t,i}). \quad (3)$$

where θ represents the model parameters, and N is the number of samples.

In DF-training, we first freeze the Transformer model's gradients to prevent parameter updates during the generation of decision feedback prompts. This process involves iterative forward passes, where the model's noisy output is incorporated into the prompt to create a new context. The generated prompts are then used to train the model and update its parameters. However, DF-training is time-intensive, as each step of detection and feedback requires a forward pass through the model. Additionally, the presence of noisy data complicates convergence, making effective training more challenging.

In contrast, when the Transformer is trained using ICL-training but tested under DF-testing conditions, a mismatch arises: the model is trained on clean data but evaluated with noisy contexts. Despite this discrepancy, we have observed that Transformer demonstrates significant robustness to noise during DF-testing and maintains acceptable performance. Furthermore, ICL-training is approximately ten times faster than DF-training, as it eliminates the need for iterative data sampling and exclusively uses clean data.

Considering all factors, our final proposed solution is to *perform ICL-training first, followed by tailored DF-training*. Here, ICL-training serves as pre-training, while tailored DF-training acts as fine-tuning, similar to the pre-training and fine-tuning processes used in LLMs. Training epochs are carefully structured into two phases, as shown in Figure 5 and Figure 6. In the first phase, the model converges just before reaching a plateau, at which point we transition to the tailored DF-training method. During this transition, a spike in the training loss is observed due to the shift in the training data distribution. As shown later, ICL pre-training not only accelerates convergence but also improves recognition of clean data and ICL-testing performance.

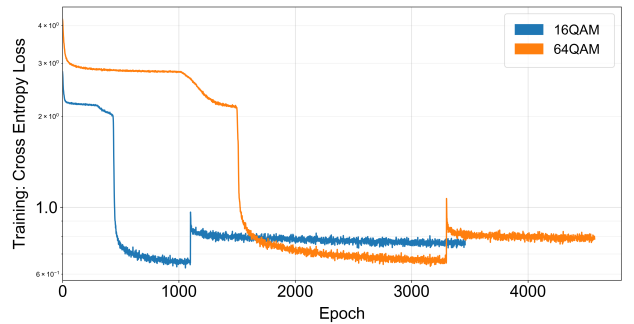


Fig. 6. Training process loss evolution. The Transformer is initially trained from scratch using ICL pre-training, followed by tailored DF fine-tuning. The training processes are shown for SISO 16QAM and 64QAM, respectively. In the first phase, the loss exhibits an initial lull where it remains constant for a period, which is typical in ICL training, before decreasing sharply. Prior to reaching a plateau, the transition to tailored DF fine-tuning introduces a spike in loss due to the data distribution shift, followed by a gradual decrease as the model converges.

3) *Decision Feedback Fine-tuning*: Instead of vanilla DF-training in the second phase, we employ a carefully designed

fine-tuning process, as illustrated in Figure 6. The loss function is formulated as a weighted combination of the previously defined losses in Equations (2) and (3), where α controls the balance between them, and the hyperparameter α is set to 0.7 during model training,

$$\mathcal{L}^{\text{fine-tuning}}(\theta) = \alpha \mathcal{L}^{\text{DF}}(\theta) + (1 - \alpha) \mathcal{L}^{\text{ICL}}(\theta). \quad (4)$$

As explained in the pre-training phase, after ICL pre-training, the model is capable of general symbol detection, performing well on detection with clean data and, to some extent, on detection using the decision feedback method. Furthermore, in the fine-tuning process, the training loss is designed to emphasize decision feedback detection while retaining the model’s ability to handle clean data.

Training on both clean and noisy data enhances the robustness of the Transformer model by exposing it to a more diverse dataset. Ultimately, we propose that a **single Transformer model** can be trained to perform both ICL-testing and DF-testing, making our DEFINED model adaptable for practical wireless systems. For example, in scenarios with sufficient pilot information, the model can operate in the ICL manner. However, in challenging situations – common in real-world applications – where pilots are limited and difficult to acquire, the model can utilize previous decisions to improve performance in subsequent symbol detection. In fact, as we will see in the experimental results, the pre-trained DEFINED model can handle previously unseen channel fading distribution very well. Remarkably, all of these generalization properties can be achieved with a single pre-trained Transformer.

VI. IN-CONTEXT SEMI-SUPERVISED LEARNING (IC-SSL)

In the previous sections, we have designed DEFINED using an approach that extends the prompt with decision pairs to improve the performance of subsequent detections. The benefits of DEFINED largely come from the *pseudo-labels* obtained from the decision pairs, which may not always be perfect. A natural question arises: *Is there a different approach to utilize the undetected received symbols to improve detection performance?*

We approach this question from the perspective of semi-supervised learning (SSL) [43]. Specifically, we propose to drop the pseudo-label and leave it null, using a semi-supervised context consisting of labeled pairs and unlabeled features. This approach allows our receiver to effectively function as an SSL estimator during inference, as illustrated in Figure 7. We hypothesize that the Transformer learns an optimal SSL estimator, enabling it to extract valuable information from unlabeled features and perform in-context semi-supervised learning during inference. This hypothesis, however, is a fundamental ML question and we leave its (dis)proof as a possible future research direction.

In this section, we first introduce the basic formulation of SSL along with its key assumptions. Then, we explain the connection to our problem formulation, introduce the new **IC-SSL model**, compare it to previous results, and illustrate how SSL operates within the Transformer during inference.

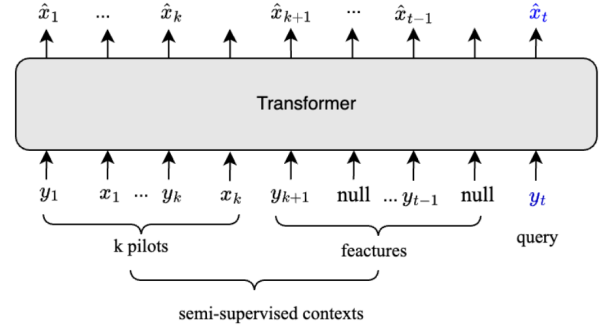


Fig. 7. IC-SSL model architecture with k pilots and $(t - k - 1)$ received signals to detect x_t , $\forall t = k + 1, \dots, T$.

Semi-supervised learning (SSL) is a machine learning paradigm that lies between supervised and unsupervised learning. It leverages a small amount of labeled data alongside a large amount of unlabeled data during model training. SSL is particularly useful when the labeled data is expensive or time-consuming to acquire, while unlabeled data is abundant and easily accessible. The core idea is that unlabeled features can enhance the understanding of the feature space even without labels, thereby aiding in the design of more effective classification boundaries and ultimately improving accuracy.

The success of SSL relies on two key assumptions about the feature space:

Assumption 1 (Clustering). *Data points in the same cluster (or manifold) are more likely to share the same label.*

Assumption 2 (Smoothness). *If two points are close in the space, their corresponding labels should also be close.*

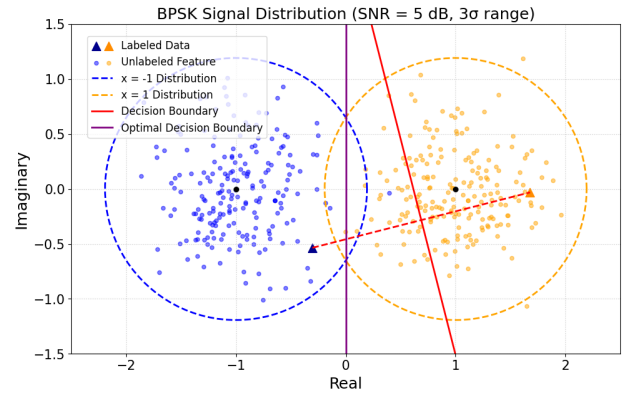


Fig. 8. Using BPSK as an example, the received signal follows a mixture of Gaussian distributions. Relying only on labeled data, the initial decision boundary (in red) is suboptimal. By incorporating unlabeled data and assuming that the data distribution is clustered and smooth, labels can be correctly propagated to neighboring features with high probability, refining the decision boundary. This shift to the optimal boundary (in purple) demonstrates the performance improvement achieved through the inclusion of unlabeled data.

The first assumption of SSL posits that features belonging to the same class tend to cluster, and the decision boundary should pass through regions of low data density rather than intersecting the clusters. The second assumption suggests that the model’s decision function should be smooth across the data distribution, meaning that if two data points are close in the input space, their corresponding labels should also be similar. In our modulation problem, the feature space follows a mixture of Gaussian distributions, with each Gaussian centered

at a constellation point and subject to Gaussian channel noise. This structure aligns with both the clustering and smoothness assumptions of SSL. As illustrated in Figure 8 using BPSK as an example, the assumptions about the received signal distribution, combined with the incorporation of unlabeled features, can effectively improve decision-making, leading to enhanced performance.

We redesign the experiment by removing the pseudo-labels and training the model using only the provided pilot pairs and unlabeled received signals. During training, the positions of the pseudo-labels are replaced with all-zero embeddings, and the same approach is applied during inference. All other training details remain the same as in the previous setup. The model, referred to as the **IC-SSL model**, uses an input prompt structured as for $t = k + 1, k + 2, \dots, T$: $S_t^{\text{SSL}} = \{y_1, x_1, \dots, y_k, x_k, y_{k+1}, \dots, y_{t-1}, y_t\}$, where the prompt contains k pilot pairs and $(t - k)$ unlabeled features. The loss function for the IC-SSL model is defined as

$$\mathcal{L}^{\text{SSL}}(\theta) = \frac{1}{N(T-k)} \sum_{i=1}^N \sum_{t=k+1}^T \text{loss}(f_\theta(S_{t,i}^{\text{SSL}}), x_{t,i}), \quad (5)$$

where f_θ represents the Transformer model with parameters θ , and the loss function is the cross-entropy loss.

VII. EXPERIMENT

We present the experimental results and analyze the performances of `DEFINED` and IC-SSL in comparison with baseline algorithms. The results suggest that our model achieves superior performance not only with sufficient pilot data but also exhibits notable improvements in limited-data scenarios by effectively leveraging noisy feedback. Furthermore, `DEFINED` demonstrates robust performance in complex modulation tasks as well as mismatched channel distributions.

A. Baseline Algorithms

We first describe several baseline algorithms, including the ICL method, the MMSE algorithm, and MMSE-DF which is a decision-feedback variant of MMSE.

1) *In-Context Learning*: We train a Transformer from scratch using vanilla ICL-training and evaluate the SER for both ICL-testing and DF-testing, shown as “ICL-ICL” and “ICL-DF” curves in the figures, respectively. Note that ICL-ICL does not utilize any decision feedback, while ICL-DF has a mismatch since the training phase does not have any decision-feedback data, but the testing phase utilizes such feedback.

2) *MMSE Algorithm*: This is a coherent detection algorithm, which first estimates the channel with the assistance of pilots and then performs detections for the subsequent received signals using the estimated channel. Assuming a known pilot signal matrix $X = [x_1, x_2, \dots, x_k]$, the received signal matrix is represented as $Y = HX + Z = [y_1, y_2, \dots, y_k]$. In the case of Rayleigh fading, both the channel and noise follow complex Gaussian distributions, and the pair (H, Y) is jointly Gaussian. The MMSE estimator for H can be derived as: $\hat{H}_k^{\text{MMSE}} = YX^\dagger(XX^\dagger + \sigma^2I)^{-1}$. When the channel fading is not Gaussian, this is the linear MMSE (LMMSE) channel

estimator. Then, with the t -th received signal y_t , the transmitted symbol x_t is estimated by projection onto the closest symbol in \mathcal{X} :

$$\hat{x}_t = \arg \min_{x \in \mathcal{X}} \|\hat{H}_k^{\text{MMSE}} x - y_t\|^2, \forall t = k + 1, \dots, T. \quad (6)$$

With k pilot pairs, the mean SER is computed and shown as a horizontal line labeled “MMSE-Pk”.

3) *MMSE-DF Algorithm*: MMSE-DF is an extension of the previous MMSE solution by sequentially using the decision feedback data as if they were new pilot pairs. Starting with k pilots, we compute the MMSE estimator of H and detect \hat{x}_{k+1} using y_{k+1} , as described in Equation (6). The decision pair (y_{k+1}, \hat{x}_{k+1}) is merged with the existing dataset and iteratively used to detect each subsequent signal until \hat{x}_T . The SER is plotted against the decision feedback-extended context sequence length.

B. Experimental Results

During testing, we randomly sample 80,000 prompts to compute the mean SER across tasks. Channel realizations follow i.i.d. Rayleigh distributions in both training and testing (except in Section VII-B6), with the difference being that in the training phase, the dataset has different SNRs as described before. Results are presented for BPSK, QPSK, 16QAM, and 64QAM in the SISO system, and for BPSK and QPSK in a 2x2 MIMO system. We note that for methods that do not utilize feedback (such as ICL-ICL), the SER is plotted as a function of the *pilot* sequence length to evaluate the impact of different numbers of pilots. For methods that utilize decision feedback (such as ICL-DF, MMSE-DF, and `DEFINED`), SER is plotted as a function of the *context* sequence length. In this case, we emphasize that the adopted number of pilots is fixed, and we increase the context length by iteratively adding detected symbols. Specifically, the t -th point represents the SER of the estimator \hat{x}_{t+1} using t contexts, omitting the 0-th point. A glossary summarizing key training and testing configurations is provided in Table I for clarity.

To quantify the SER improvement with increasing context length under DF-testing, we define the gain metric as:

$$\text{gain}_{\text{DF}} = \left(\frac{\text{SER}_k(\theta) - \text{SER}_{T-1}(\theta)}{\text{SER}_k(\theta)} \right) \times 100\%, \quad (7)$$

which represents the percentage reduction in SER as the context length increases from k to $(T - 1)$, starting from k known pilots.

1) *Comparison with Baseline Algorithms under DF-testing*: We first compare `DEFINED` with the baseline algorithms under DF-testing in scenarios with *extremely limited* pilot data: a **single pilot** in the SISO system and **two pilots** in the 2x2 MIMO system. The results are presented in Figure 9.

The `DEFINED` lines represent the performance of our proposed model during DF-testing, demonstrating a significant reduction in SER as more decision feedback data is incorporated, i.e., increased context sequence lengths. For instance, in Figure 9c, for 16QAM with one pilot, the SER decreases from 0.135 to 0.076 as the feedback context sequence length increases, achieving a 0.437 SER gain. Remarkably, our model

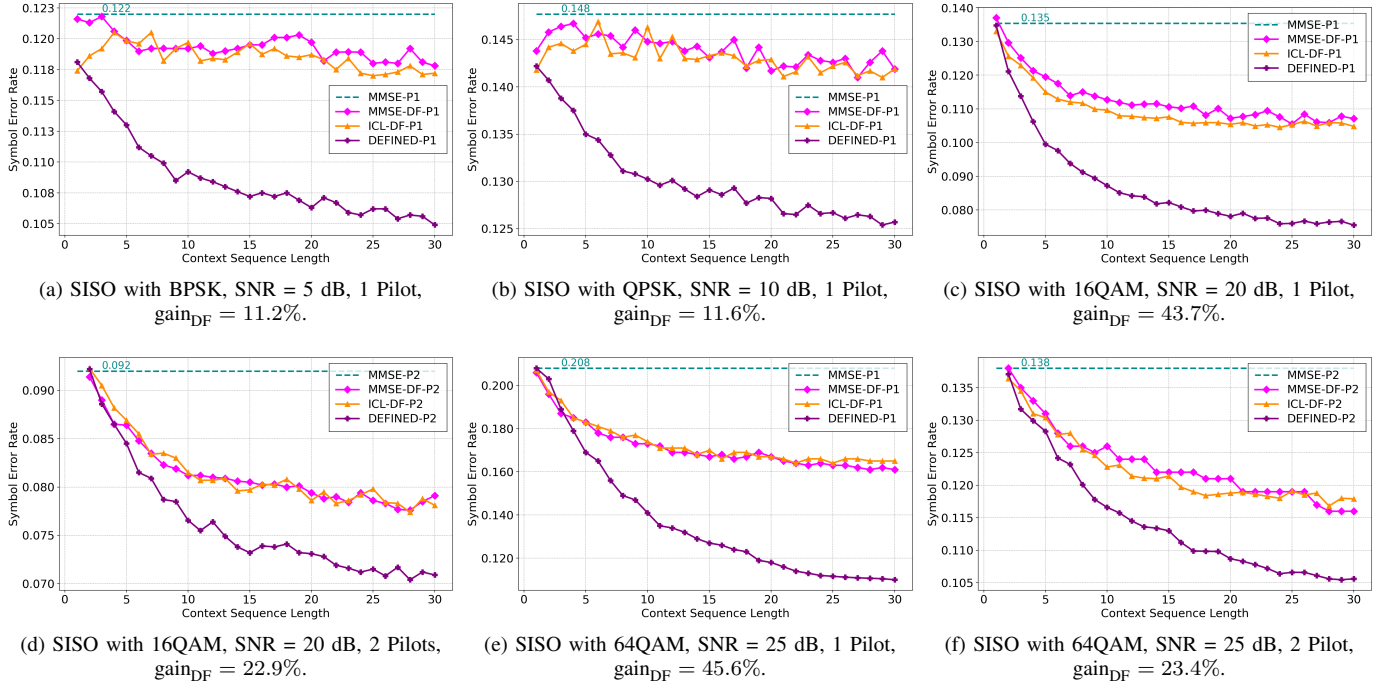


Fig. 9. SER as a function of context sequence length for SISO systems with BPSK, QPSK, 16QAM, and 64QAM under varying SNRs and pilot lengths.

TABLE I
GLOSSARY OF TRAINING AND TESTING METHODS

Term	Description
ICL-training	Training with only clean pilot sequences.
DF-training	Training with decision feedback sequences.
ICL-testing	Testing with clean pilots only.
DF-testing	Testing with decision feedback prompts.
Pilot Sequence Length	Number of pilots.
Context Sequence Length	Total sequence length, including feedback.
ICL (ICL-ICL)	ICL-trained, ICL-tested (no feedback).
ICL-DF	ICL-trained, DF-tested (mismatch).
DEFINED (DEFINED-DF)	DF-trained, DF-tested.
DEFINED-ICL	DF-trained, ICL-tested.
MMSE-Pk	MMSE with k pilots (baseline).
MMSE-DF	MMSE with decision feedback.

achieves performance comparable to conventional methods requiring over 4 pilot pairs while using only a single pilot pair. This confirms that the Transformer effectively utilizes noisy feedback to improve detection performance with limited pilot data.

The ICL-DF line, which represents a Transformer trained with the ICL method but tested using decision feedback as if the detected symbols are pilots, performs significantly worse than our model, nearly coinciding with the MMSE-DF line. This observation highlights that models trained solely on clean data struggle with noisy feedback, as they simply treat all feedback data as clean. This underscores the importance of DF fine-tuning to effectively handle noisy feedback.

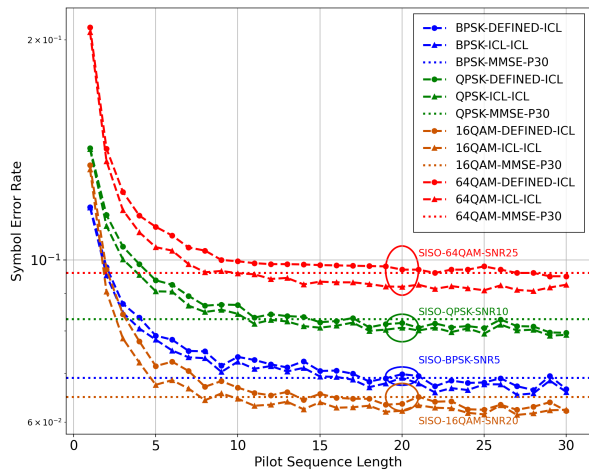
2) *Comparison with Baseline Algorithms Without Decision Feedback:* We then compare our DEFINED model with baseline algorithms under ICL-testing (i.e., no DF). Complete results are grouped according to cases in SISO and MIMO systems under specific modulation schemes and SNR levels, as shown in Figure 10. The ICL-ICL line, representing the

model trained and tested using the ICL method, demonstrates that with 30 pilots, the Transformer slightly outperforms the MMSE algorithm with 30 pilots during ICL testing. This improvement arises from the model’s ability to jointly perform channel estimation and symbol detection, leveraging the synergy between these tasks.

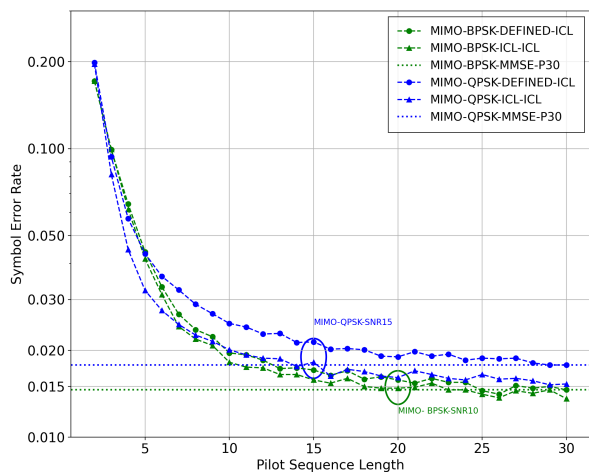
Importantly, DEFINED also performs well in ICL testing, as indicated by the DEFINED-ICL line, which closely aligns with the ICL-ICL line. This result suggests that ICL pre-training, followed by carefully designed loss functions during decision feedback fine-tuning, also enables the model to effectively learn from clean data. Additionally, together with the results from DF-testing, we demonstrate that **a single pre-trained Transformer can perform both DF and no-DF tasks**. Our DEFINED model adapts well to real-world symbol detection scenarios, excelling with ample pilot data and maintaining strong performance even with a single pilot.

3) *Comparison with Different SNRs and Varying Pilot Lengths:* At high SNR levels, reduced data noise enables more accurate detections from pilot data, enhancing DEFINED model performance and accentuating the downward SER trend. However, at very high SNRs, the already low initial SER limits further improvement. Our DEFINED model also performs robustly with minimal pilot data, including the extreme single-pilot cases. As pilot length increases, as shown in Figures 9d and 9f, all algorithms exhibit improved performance in DF inference.

4) *Comparison with Different Modulation Schemes:* We conduct experiments using BPSK, QPSK, 16QAM, and 64QAM modulations in the SISO system, representing classification tasks with 2, 4, 16, and 64 classes, respectively. As modulation complexity increases, the detection task becomes more challenging, but we observe greater performance improvements with complex schemes, as reflected by a more



(a) ICL-testing performance in the SISO system.



(b) ICL-testing performance in the MIMO system.

Fig. 10. SER as a function of pilot sequence length under ICL-testing conditions, comparing DEFINED and vanilla ICL models in SISO and MIMO systems across various modulation schemes.

pronounced SER decrease with additional feedback data in our DEFINED model.

Analysis of the Transformer’s output logit vector shows that nearly all of the incorrect detections occur within a small region around the ground-truth label in the constellation. This “typical error event” [38] suggests that even incorrect detections carry valuable information, *as the noisy label is often near the correct one, enhancing the model’s detections*. Thus, as modulation complexity increases, the compact constellation set allows noisy feedback to provide more useful information, leading to better SER gains with added feedback data.

These findings demonstrate that our DEFINED model effectively captures the constellation set’s geometry. It not only learns detections but also recognizes relationships between classes, often assigning higher probabilities to neighboring labels when errors occur. Due to inherent data noise – e.g., channel fading and additive noise – received signals with nearby latent labels in the constellation may overlap. As a result, the model sees adjacent labels as close neighbors, letting its detections retain valuable information, even when they are not entirely accurate.

5) *MIMO Results*: The results for MIMO systems with BPSK and QPSK using two pilots are shown in Figure 11. Compared across different modulation schemes, SNR levels, our DEFINED model can still perform well for high-dimensional detection problems. In fact, DEFINED exhibits a more pronounced decrease in SER with the inclusion of additional decision feedback data, leveraging the underlying communication system structure more effectively.

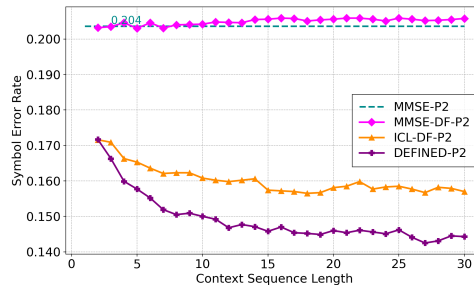
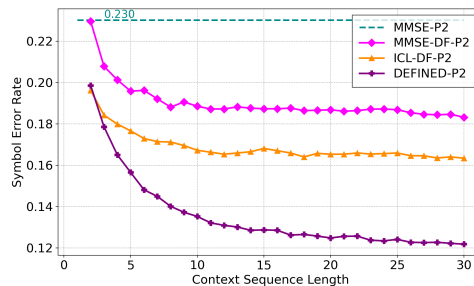
(a) MIMO with BPSK, SNR = 10 dB, 2 Pilots, $\text{gain}_{\text{DF}} = 16.8\%$.(b) MIMO with QPSK, SNR = 15 dB, 2 Pilots, $\text{gain}_{\text{DF}} = 38.6\%$.

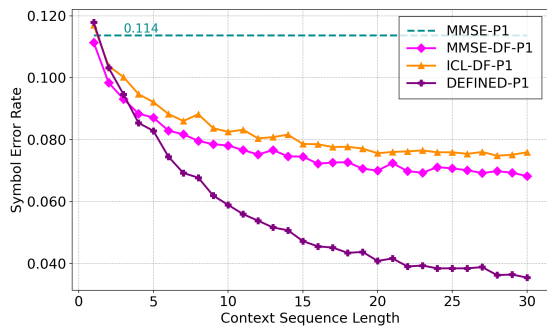
Fig. 11. SER as a function of context sequence length for MIMO systems with BPSK and QPSK under varying SNR levels and 2 pilots.

6) *Robustness to Channel Distribution Mismatch*: We evaluate the robustness of our DEFINED model under channel distribution mismatches. Specifically, we consider a DEFINED model trained on a SISO 64QAM system with a single pilot and SNRs uniformly sampled from [20, 25] dB, consistent with the previous experiment.

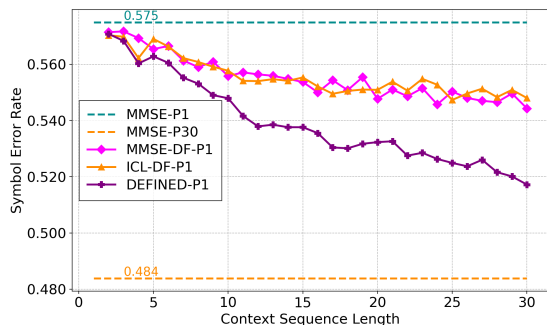
First, the model is trained on a Rayleigh fading channel without a line-of-sight (LOS) component, $H_{\text{train}} \sim \mathcal{CN}(0, I)$, and tested on a Rician fading channel with an LOS component at SNR = 25 dB: $H_{\text{test}} \sim \sqrt{\frac{\kappa}{\kappa+1}} e^{j\theta} + \sqrt{\frac{1}{\kappa+1}} \mathcal{CN}(0, I)$, where $\kappa = 4$ represents the LOS-to-NLOS power ratio, modeling suburban or rural environments [38], and θ is uniformly sampled to reflect varying LOS conditions. As shown in Figure 12a, DEFINED remains robust despite the channel mismatch, benefiting from the additional LOS component, which reduces the SER from 0.117 to 0.036.

Second, we evaluate a more challenging scenario where the model is tested in a Rayleigh fading channel with two pilots at SNR = 15 dB (which is below the range of SNRs in the training), introducing increased noise and pilot mismatch. As shown in Figure 12b, DEFINED achieves a 10.1% SER gain, reducing the SER from 0.573 to 0.515. In this extremely noisy condition, MMSE-P30, which uses 30 pilots, achieves an SER of 0.484. This highlights the adaptability of DEFINED

to varying pilots and noise levels, demonstrating its robustness under adverse conditions.



(a) SISO Rician 64QAM, SNR = 25 dB, 1 Pilot, $\text{gain}_{\text{DF}} = 71.1\%$.



(b) SISO Rayleigh 64QAM, SNR = 15 dB, 2 Pilots, $\text{gain}_{\text{DF}} = 10.1\%$.

Fig. 12. Performance under channel distribution mismatch.

C. Comparison with Non-Coherent Detection

Here, we compare DEFINED with a non-coherent detection algorithm, which also does not explicitly perform channel estimation.

1) Maximum Likelihood Sequence Detection Algorithm:

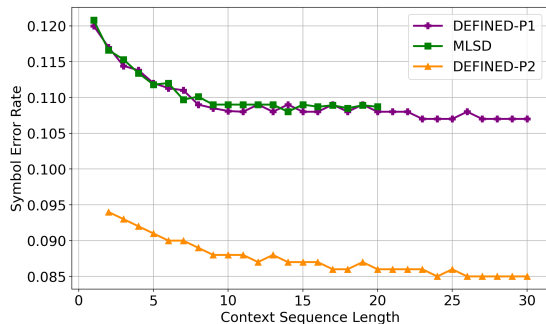
We consider a non-coherent detection algorithm [44] for the block fading channel in the SISO system, which does not require explicit channel estimation. Maximum Likelihood sequence detection (MLSD) is optimal in terms of minimizing the *sequence* error rate on the entire received signal sequence. Given the received signal sequence $Y = [y_1, y_2, \dots, y_T]$, the MLSD outputs the sequence $S = [s_1, s_2, \dots, s_T]$ that maximizes the conditional probability density function of Y given S . The optimal decision is given by: $S^{\text{MLSD}} = \arg \max_{S \in \mathcal{X}^T} f(Y|S)$, where $f(Y|S)$ represents the probability density function (PDF) of the channel output conditioned on the transmitted symbol sequence. We consider the Rayleigh block fading channel $H \sim \mathcal{CN}(0, 1)$ and channel noise $Z = [z_1, z_2, \dots, z_T]$ with zero mean and covariance matrix $\sigma^2 I$. Thus, S^{MLSD} can be written as [44]:

$$S^{\text{MLSD}} = \arg \max_{S \in \mathcal{X}^T} \left\{ \frac{|SY^\dagger|^2}{\sigma^2 \|S\|^2 + \sigma^4} - \ln(\|S\|^2 + \sigma^2) \right\}. \quad (8)$$

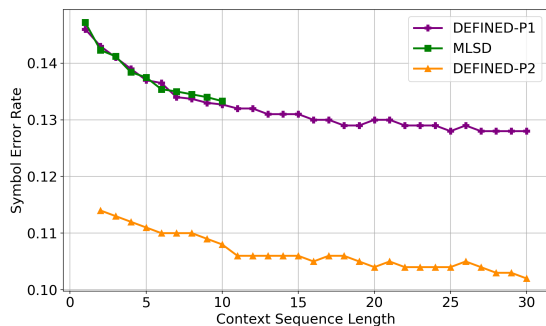
Two forms of ambiguity exist in this non-coherent detection problem. The first is *phase ambiguity*, which occurs for any constellation invariant under a specific phase rotation. The second is *divisor ambiguity*, which arises when multiple points

lie on the same one-dimensional subspace [45]. For SISO scenarios with BPSK and QPSK, since all constellation points lie on the unit circle, the second ambiguity does not exist. The first ambiguity can be resolved by using the phase of the last symbol from the previous block, as described in [46]. Practically, this is achieved by overlapping successive blocks by one symbol and using the last symbol of the previous block as the reference for the current block.

In our experiment, phase ambiguity is resolved by knowing the phase of the first symbol in the transmitted sequence at the receiver and searching for the optimal S^{MLSD} within the subspace of \mathcal{X}^T . The average SER is then calculated for the remaining $(T - 1)$ symbols, as the phase of the first symbol is known for a coherent interval of length T . Moreover, knowing the phase of the first symbol in SISO BPSK and QPSK scenarios is almost equivalent to having one pilot and is analogous to the setup used in previous baseline algorithms, which include one pilot and a total decision feedback enhanced context sequence of length $(T - 1)$. This ensures a relatively fair comparison between the methods. Consequently, we enumerate T from 2 to 31, compute the mean SER over tasks for detecting a sequence of T received signals, and plot it at the index corresponding to a context sequence length of $(T - 1)$ in the following results.



(a) SISO with BPSK, SNR = 5 dB



(b) SISO with QPSK, SNR = 10 dB

Fig. 13. Comparison of the DEFINED model with 1 and 2 pilots and the MLSD algorithm in SISO systems for BPSK and QPSK.

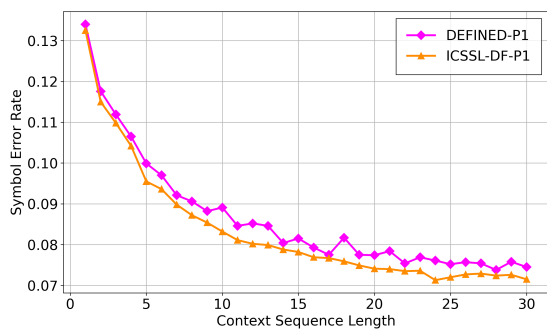
2) *Results:* As shown in Figure 13, we compare the performance of the non-coherent MLSD algorithm with our DEFINED model in the SISO system using BPSK and QPSK modulations. The implementation of efficient MLSD algorithms has been an active area of research for decades [44]. However, since the problem is fundamentally NP-hard, computationally efficient algorithms often suffer from performance

degradation (albeit small in some settings). We thus implement MLSD using an exhaustive search for varying sequence lengths. As the computational complexity grows *exponentially* with the sequence length, we only report the feasible results within some reasonable timeframe.

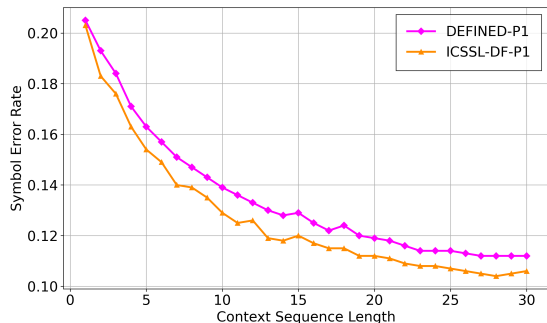
The DEFINED-P1 curves demonstrate that our model’s performance with one pilot under DF-testing matches that of the MLSD detector, which is the optimal sequence estimator with the additional first symbol phase information (almost equivalent to one pilot). Furthermore, with two pilots, our DEFINED model significantly outperforms the MLSD detector, as DEFINED directly minimizes the SER, as shown by the DEFINED-P2 line. The adaptability of DEFINED allows it to smoothly transition between non-coherent and coherent detection modes while consistently benefiting from decision feedback data.

Our experiment results demonstrate that DEFINED with one pilot empirically aligns with the MLSD estimator at short sequence lengths. This empirical finding aligns with previous theoretical results on ICL [25], [26], [42]. Practically, although DEFINED achieves similar or slightly better performance than MLSD during a single forward pass, we can avoid the exponentially increasing computational complexity associated with a true MLSD. Moreover, as the number of pilot pairs increases, DEFINED smoothly transitions to coherent detection and significantly outperforms the MLSD detector. Additionally, the true data distribution is often infeasible to obtain in real-world scenarios, making MLSD detection challenging to implement. In contrast, data-driven methods like Transformers show great potential in wireless communication tasks.

D. IC-SSL Results



(a) IC-SSL SISO with 16QAM, SNR = 20 dB



(b) IC-SSL SISO with 64QAM, SNR = 25 dB

Fig. 14. In-context semi-supervised learning in a SISO system with 16QAM and 64QAM.

We compare the performance of our IC-SSL model with the previous DEFINED model in Section V. As shown in Figure 14, for the relatively difficult modulation schemes (16QAM and 64QAM) in the SISO system, the IC-SSL model performs similarly or slightly better than the DEFINED model. This demonstrates that even without the pseudo-labels, the performance improvement over ICL remains consistent. It also shows that the Transformer jointly extracts information from both labeled data pairs and unlabeled features, gaining a better understanding of the feature space from the unlabeled data. Given the clustered and smooth nature of the feature distribution, the model can establish a more optimal classification decision boundary, leading to improved SER in subsequent decision-making, effectively performing SSL during inference.

On the other hand, the DEFINED model, which undergoes ICL pre-training followed by DF fine-tuning, ultimately achieves similar performance as the IC-SSL model in DF-testing. This reveals that the model acquires general capabilities akin to supervised learning during ICL pre-training, while DF fine-tuning effectively transitions the model from supervised to semi-supervised learning, even with the inclusion of pseudo-labels. This is enabled by the Transformer’s self-attention mechanism, which assigns varying weights to different parts of the input sequence for each output embedding, allowing the model to focus automatically on the most relevant information. We conjecture that during DF fine-tuning, the attention parameters are adjusted to prioritize the unlabeled features over the pseudo-labels, explaining the initial spike and gradual decrease in loss observed during fine-tuning, as shown in Figure 6.

Unlike previous studies on ICL, where prompts consist solely of feature-label pairs and Transformers are employed to learn mappings between them, our IC-SSL model generalizes the prompt by incorporating unlabeled features. This approach demonstrates that Transformers, beyond the conventional supervised learning paradigm, are remarkably powerful in extracting information and learning SSL mappings. This innovation significantly extends the applicability of Transformers beyond this particular wireless communication task.

VIII. CONCLUSIONS

In this work, we proposed the DEFINED framework, inspired by decision feedback in wireless communication, to enhance symbol detection by incorporating decision pairs into prompts. Our approach achieved significant performance gains with limited pilot data while maintaining high accuracy with sufficient pilot data, making it highly adaptable for practical scenarios. Additionally, we introduced the IC-SSL model, demonstrating that Transformers could leverage both labeled data and unlabeled features for effective semi-supervised learning during inference. Extensive experiments across various modulation schemes in both SISO and MIMO systems validated the robustness and adaptability of our models. These contributions highlighted the potential of Transformers to perform both supervised and semi-supervised in-context learning, underscoring their suitability for future wireless communication systems. Furthermore, we conjecture that our

DEFINED model learns the optimal semi-supervised estimator, a direction that warrants further theoretical investigation.

REFERENCES

- [1] O. Simeone, S. Park, and J. Kang, "From learning to meta-learning: Reduced training overhead and complexity for communication systems," in *2020 2nd 6G Wireless Summit (6G SUMMIT)*. IEEE, 2020, pp. 1–5.
- [2] C. Finn, P. Abbeel, and S. Levine, "Model-agnostic meta-learning for fast adaptation of deep networks," in *International conference on machine learning*. PMLR, 2017, pp. 1126–1135.
- [3] L. Chen, S. T. Jose, I. Nikoloska, S. Park, T. Chen, O. Simeone *et al.*, "Learning with limited samples: Meta-learning and applications to communication systems," *Foundations and Trends® in Signal Processing*, vol. 17, no. 2, pp. 79–208, 2023.
- [4] S. Park, H. Jang, O. Simeone, and J. Kang, "Learning to demodulate from few pilots via offline and online meta-learning," *IEEE Trans. Signal Processing*, vol. 69, pp. 226–239, 2020.
- [5] A. Vaswani, N. Shazeer, N. Parmar, J. Uszkoreit, L. Jones, A. N. Gomez, L. Kaiser, and I. Polosukhin, "Attention is all you need," *Advances in Neural Information Processing Systems*, 2017.
- [6] A. Radford, J. Wu, R. Child, D. Luan, D. Amodei, I. Sutskever *et al.*, "Language models are unsupervised multitask learners," *OpenAI blog*, vol. 1, no. 8, p. 9, 2019.
- [7] B. Mann *et al.*, "Language models are few-shot learners," in *Advances in Neural Information Processing Systems*, H. Larochelle, M. Ranzato, R. Hadsell, M. Balcan, and H. Lin, Eds., vol. 33. Curran Associates, Inc., 2020, pp. 1877–1901.
- [8] S. Garg, D. Tsipras, P. S. Liang, and G. Valiant, "What can transformers learn in-context? a case study of simple function classes," *Advances in Neural Information Processing Systems*, vol. 35, 2022.
- [9] V. Teja Kunde, V. Rajagopalan, C. Shekhara Kaushik Valmееkam, K. Narayanan, S. Shakkottai, D. Kalathil, and J.-F. Chamberland, "Transformers are provably optimal in-context estimators for wireless communications," *arXiv e-prints*, pp. arXiv:2311.2023.
- [10] M. Zecchin, K. Yu, and O. Simeone, "In-context learning for MIMO equalization using transformer-based sequence models," in *2024 IEEE International Conference on Communications Workshops (ICC Workshops)*. IEEE, 2024, pp. 1573–1578.
- [11] —, "Cell-free multi-user MIMO equalization via in-context learning," in *IEEE International Workshop on Signal Processing Advances in Wireless Communications (SPAWC)*. IEEE, 2024, pp. 646–650.
- [12] M. Abbas, K. Kar, and T. Chen, "Leveraging large language models for wireless symbol detection via in-context learning," *arXiv preprint arXiv:2409.00124*, 2024.
- [13] F. Liang, C. Shen, and F. Wu, "An iterative BP-CNN architecture for channel decoding," *IEEE J. Sel. Topics Signal Process.*, vol. 12, no. 1, pp. 144–159, February 2018.
- [14] F. Liang, C. Shen, W. Yu, and F. Wu, "Towards optimal power control via ensembling deep neural networks," *IEEE Trans. Commun.*, vol. 68, no. 3, pp. 1760–1776, March 2020.
- [15] O. Simeone, "A very brief introduction to machine learning with applications to communication systems," *IEEE Trans. Cogn. Commun. Netw.*, vol. 4, no. 4, pp. 648–664, 2018.
- [16] K. Yang, C. Shi, C. Shen, J. Yang, S. Yeh, and J. Sydir, "Advancing RAN slicing with offline reinforcement learning," in *IEEE DySPAN*, May 2024, pp. 1–6.
- [17] —, "Offline reinforcement learning for wireless network optimization with mixture datasets," *IEEE Trans. Wireless Commun.*, vol. 23, no. 10, pp. 12 703–12 716, October 2024.
- [18] K. Yang, J. Yang, and C. Shen, "Average reward reinforcement learning for wireless radio resource management," in *Asilomar Conference on Signals, Systems, and Computers*, October 2024, pp. 1–6.
- [19] M. Baur, B. Fesl, M. Koller, and W. Utschick, "Variational autoencoder leveraged MMSE channel estimation," in *2022 56th Asilomar Conference on Signals, Systems, and Computers*. IEEE, 2022, pp. 527–532.
- [20] A. Caciularu and D. Burshtein, "Unsupervised linear and nonlinear channel equalization and decoding using variational autoencoders," *IEEE Trans. Cogn. Commun. Netw.*, vol. 6, no. 3, pp. 1003–1018, 2020.
- [21] A. Le Ha, T. Van Chien, T. H. Nguyen, W. Choi *et al.*, "Deep learning-aided 5G channel estimation," in *International Conference on Ubiquitous Information Management and Communication (IMCOM)*. IEEE, 2021.
- [22] D. Neumann, T. Wiese, and W. Utschick, "Learning the MMSE channel estimator," *IEEE Trans. Signal Processing*, vol. 66, no. 11, pp. 2905–2917, 2018.
- [23] C. Lu, W. Xu, H. Shen, J. Zhu, and K. Wang, "MIMO channel information feedback using deep recurrent network," *IEEE Commun. Letter*, vol. 23, no. 1, pp. 188–191, 2018.
- [24] F. A. Aoudia and J. Hoydis, "End-to-end learning for ofdm: From neural receivers to pilotless communication," *IEEE Trans. Wireless Commun.*, vol. 21, no. 2, pp. 1049–1063, 2021.
- [25] M. Panwar, K. Ahuja, and N. Goyal, "In-context learning through the bayesian prism," in *International Conference on Learning Representations*, 2023.
- [26] A. Raventós, M. Paul, F. Chen, and S. Ganguli, "Pretraining task diversity and the emergence of non-bayesian in-context learning for regression," *Advances in Neural Information Processing Systems*, 2024.
- [27] J. Von Oswald, E. Niklasson, E. Randazzo, J. Sacramento, A. Mordvintsev, A. Zhmoginov, and M. Vladymyrov, "Transformers learn in-context by gradient descent," in *International Conference on Machine Learning*. PMLR, 2023, pp. 35 151–35 174.
- [28] K. Ahn, X. Cheng, H. Daneshmand, and S. Sra, "Transformers learn to implement preconditioned gradient descent for in-context learning," *Advances in Neural Information Processing Systems*, vol. 36, 2023.
- [29] S. Chan, A. Santoro, A. Lampinen, J. Wang, A. Singh, P. Richmond, J. McClelland, and F. Hill, "Data distributional properties drive emergent in-context learning in transformers," *Advances in Neural Information Processing Systems*, vol. 35, pp. 18 878–18 891, 2022.
- [30] S. Min, X. Lyu, A. Holtzman, M. Artetxe, M. Lewis, H. Hajishirzi, and L. Zettlemoyer, "Rethinking the role of demonstrations: What makes in-context learning work?" in *EMNLP*, 2022.
- [31] J. Shao, J. Tong, Q. Wu, W. Guo, Z. Li, Z. Lin, and J. Zhang, "WirelessLLM: Empowering large language models towards wireless intelligence," *arXiv preprint arXiv:2405.17053*, 2024.
- [32] J. Tong, J. Shao, Q. Wu, W. Guo, Z. Li, Z. Lin, and J. Zhang, "Wirelessagent: Large language model agents for intelligent wireless networks," *arXiv preprint arXiv:2409.07964*, 2024.
- [33] J. Ott, J. Pirkil, M. Stahlke, T. Feigl, and C. Mutschler, "Radio foundation models: Pre-training transformers for 5G-based indoor localization," *arXiv preprint arXiv:2410.00617*, 2024.
- [34] N. Rashvand, K. Witham, G. Maldonado, V. Katariya, N. Marer Prabhu, G. Schirner, and H. Tabkhi, "Enhancing automatic modulation recognition for iot applications using transformers," *IoT*, vol. 5, no. 2, pp. 212–226, 2024.
- [35] W. Zhang, Y. Wang, X. Chen, Z. Cai, and Z. Tian, "Spectrum transformer: An attention-based wideband spectrum detector," *IEEE Trans. Wireless Commun.*, 2024.
- [36] Z. Song, O. Simeone, and B. Rajendran, "Neuromorphic in-context learning for energy-efficient MIMO symbol detection," *arXiv preprint arXiv:2404.06469*, 2024.
- [37] W. Kong, X. Jiao, Y. Xu, B. Zhang, and Q. Yang, "A transformer-based contrastive semi-supervised learning framework for automatic modulation recognition," *IEEE Trans. Cogn. Commun. Netw.*, vol. 9, no. 4, pp. 950–962, 2023.
- [38] D. Tse and P. Viswanath, *Fundamentals of Wireless Communication*. Cambridge University Press, 2005.
- [39] C. Shen and M. P. Fitz, "MIMO-OFDM beamforming for improved channel estimation," *IEEE J. Select. Areas Commun.*, vol. 26, no. 6, pp. 948–959, August 2008.
- [40] Z. Chen, Z. He, K. Niu, and Y. Rong, "Neural network-based symbol detection in high-speed OFDM underwater acoustic communication," in *2018 10th International Conference on Wireless Communications and Signal Processing (WCSP)*. IEEE, 2018, pp. 1–5.
- [41] H. Kim, S. Kim, H. Lee, C. Jang, Y. Choi, and J. Choi, "Massive MIMO channel prediction: Kalman filtering vs. machine learning," *IEEE Trans. Commun.*, vol. 69, no. 1, pp. 518–528, 2020.
- [42] W. Shen, R. Zhou, J. Yang, and C. Shen, "On the training convergence of transformers for in-context classification," *arXiv preprint arXiv:2410.11778*, 2024.
- [43] X. Yang, Z. Song, I. King, and Z. Xu, "A survey on deep semi-supervised learning," *IEEE Transactions on Knowledge and Data Engineering*, vol. 35, no. 9, pp. 8934–8954, 2022.
- [44] D. S. Papaliopoulos, G. Abou Elkheir, and G. N. Karystinos, "Maximum-likelihood noncoherent pam detection," *IEEE Trans. Commun.*, vol. 61, no. 3, pp. 1152–1159, 2013.
- [45] D. J. Ryan, I. V. L. Clarkson, and I. B. Collings, "Blind detection of pam and qam in fading channels," *IEEE Trans. Info. Theory*, vol. 52, no. 3, pp. 1197–1206, 2006.
- [46] R.-R. Chen, R. Koetter, U. Madhoo, and D. Agrawal, "Joint noncoherent demodulation and decoding for the block fading channel: A practical framework for approaching shannon capacity," *IEEE Trans. Commun.*, vol. 51, no. 10, pp. 1676–1689, 2003.